Electronic Supplementary Material (ESI) for Journal of Materials Chemistry C.

Supplementary Information

Fermi level pinned molecular donor/acceptor junctions: reduction of induced carrier density by interfacial charge transfer complexes

Paul Beyer,[1] Eduard Meister,[2] Timo Florian,[1] Alexander Generalov,[3]
Wolfgang Brütting,[2] Norbert Koch,[1,4] and Andreas Opitz[1]

[1] Institut für Physik & IRIS Adlershof, Humboldt-Universität zu Berlin, Germany

[2] Institute of Physics, University of Augsburg, Germany

[3] Max IV Laboratory, Lund University, Sweden

[4] Helmholtz-Zentrum Berlin für Materialien und Energie GmbH, Germany

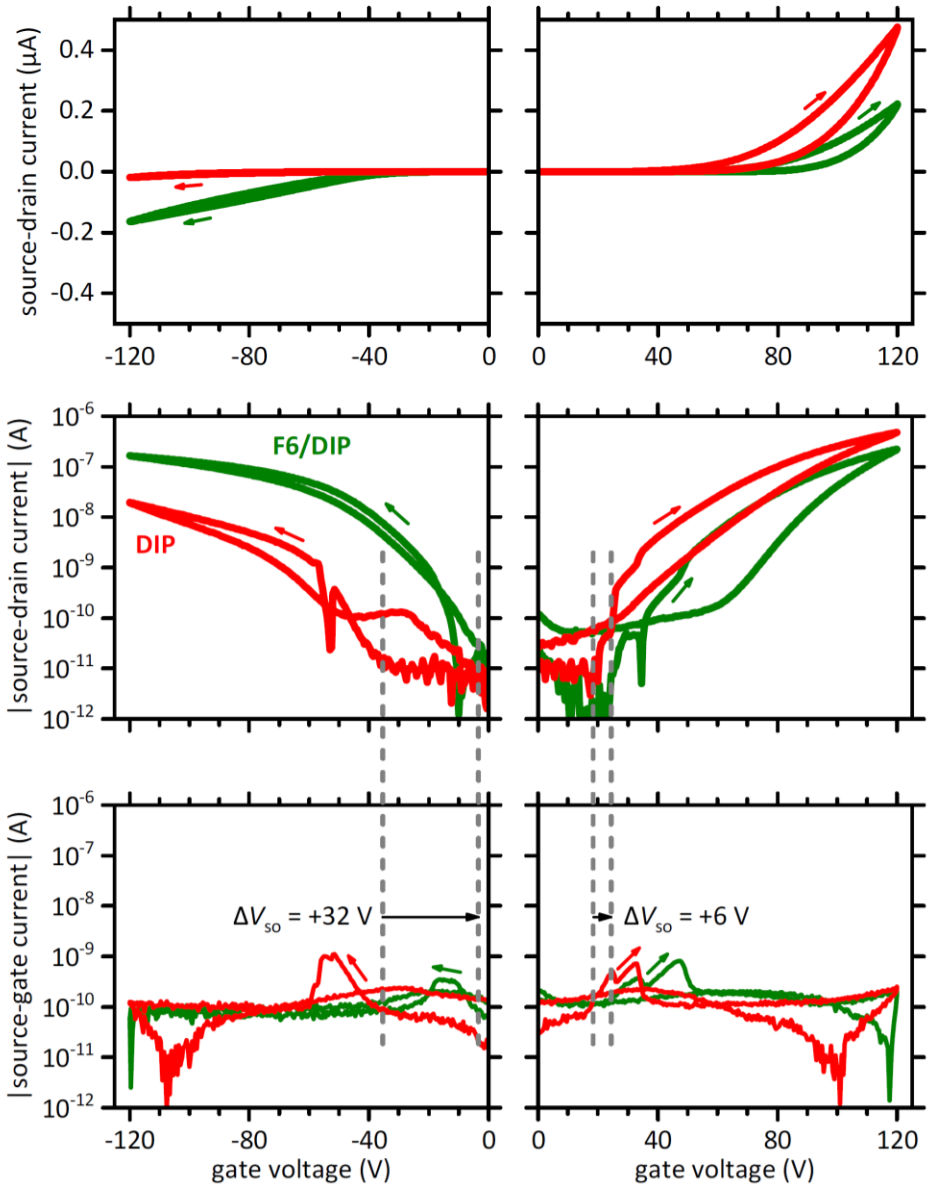

Figure S1: Source-drain current versus gate voltage (top panels: linear scale, centre panels: logarithmic scale of absolute values), as shown in the main manuscript (**Figure 2**), and the corresponding source-gate currents (bottom panels). The drop in source-drain current, at −53 V and at +35V, is due to the change of accumulation from majority to minority charge carriers and thus the sign of the current near low absolute values. Charge carrier injection and formation of a conductive channel starts at the onset of the displacement current (bottom panels) in the forward scanning direction marked with dashed vertical lines. The arrows mark the scan directions. This onset correlates well with the switch-on voltage and is therefore used to determine switch-on voltage shift ΔV_{SO}. [1]

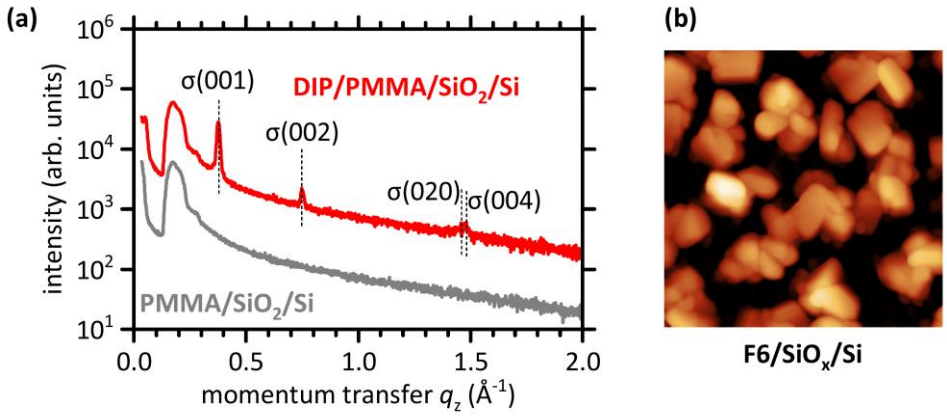

Figure S2: (a) Specular X-ray reflectivity of 50 nm DIP (top graph) deposited on a PMMA/SiO_2/Si (oxide layer thickness is 300 nm) substrate as used for the OFET fabrication. An uncovered PMMA/SiO_2/Si substrate (bottom graph) as reference shows no crystalline reflections. The scans are shifted vertically for visual clarity. X-ray diffraction measurements were taken in Θ-2Θ geometry. (b) Scanning force micrograph (2×2 µm²) of F6 deposited on native oxide (SiO_x) covered Si wafer.

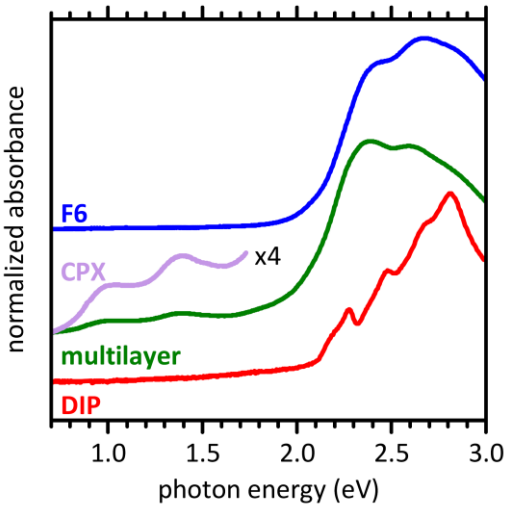

Figure S3: Optical absorption spectra of the pristine layers of DIP and F6 as well as a multilayer stack of DIP/F6/DIP…F6/DIP with 10 DA interfaces. The absorption signal related to the formed CPX is displayed as magnification and comparable to measurements on co-deposited films of DIP and F6. [2]

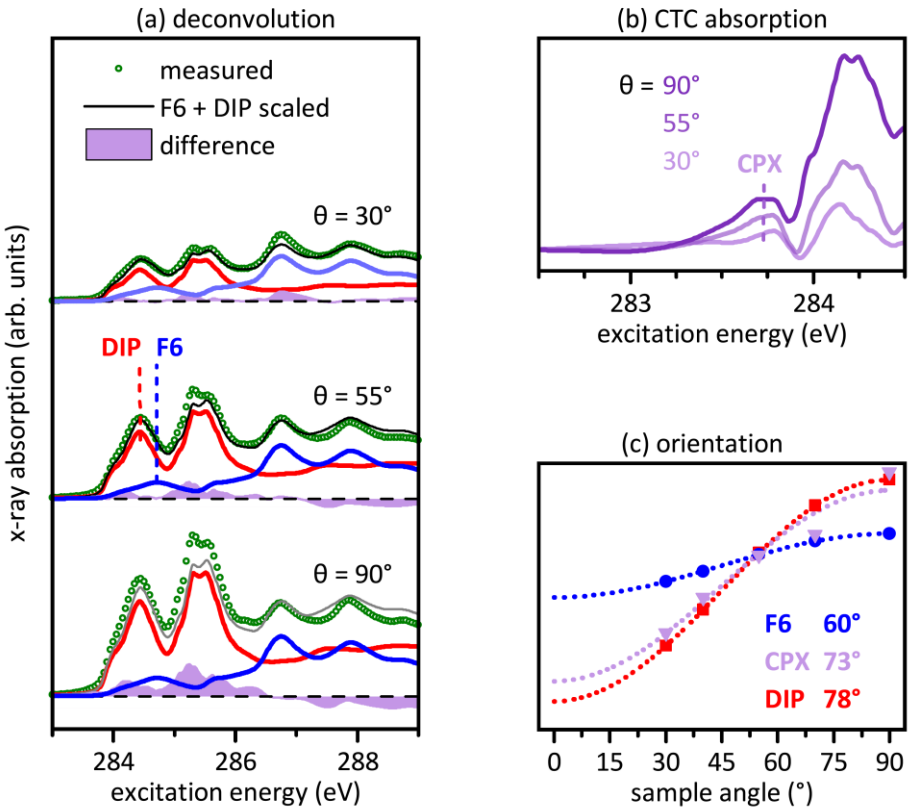

Figure S4: C1s X-ray absorption spectra (NEXAFS) of 8.5 nm F6 on top of DIP (left panel, dark green circles) for varying polar angles Θ between the photon beam and the sample plane (Θ = 90° – normal incidence, Θ = 30° – grazing incidence). For clarity, only three absorption spectra are shown here. The deconvolution into the DIP and the F6 content as well as the remaining difference related to the formed CPX are given. A magnified view of the obtained CPX absorption is shown in the right panel. The average molecular orientation of the DIP layer, the CPX layer, and the F6 top layer were determined independently of each other.[3] For this, the dichroism was analysed at different energies, as indicated by the dashed vertical lines. The intensity dependence on the angle between sample surface and incoming x-ray beam (sample angle) is given in part (c) of the figure. The doted lines in (c) are fits according to the equation given by Stöhr [3] for a threefold or higher symmetry.

Table S1: Parameters used for the calculations of the charge distributions in the differently layered stacks using the electrostatic calculations introduced in [4,5] (shown in Figure 6). The HOMO and LUMO values are derived in the main text and referenced to the vacuum level. Note that the values given here are onset values. g_{HOMO} and g_{LUMO} are the (spin-)degeneracies. The standard deviation σ is assumed to be equal for HOMO and LUMO and taken from the UPS measurements in the main text. d is the thickness of a monolayer of material, n is the number of molecules per unit area and ε_r the relative permittivity. For all peaks the shape of a Gaussian distribution was assumed. The substrate work function was set to 4.1 eV.

compound	*IE* (eV)	*EA* (eV)		g_{HOMO}, g_{LUMO}	$\sigma_{HOMO}, \sigma_{LUMO}$ (eV)	*d* (nm)	*n* (nm^{-2})	ε_r
insulator	−11.0	−0.50		2	0.2	20 nm	—	2
DIP	−5.40	−2.80	[6,7]		0.2	1.68	3.30	4
CPX	−6.10	−4.90			0.3	1.42	2.09	
F6	−7.55	−5.60	[8]		0.2	1.18	2.59	

References

[1] Y. Liang, Examination of transient carrier behaviors in organic field-effect devices via displacement current measurement, University of Minnesota, 2011. http://hdl.handle.net/11299/120537.

[2] G. Duva, L. Pithan, C. Zeiser, B. Reisz, J. Dieterle, B. Hofferberth, P. Beyer, L. Bogula, A. Opitz, S. Kowarik, A. Hinderhofer, A. Gerlach, F. Schreiber, Thin-Film Texture and Optical Properties of Donor/Acceptor Complexes. Diindenoperylene/F6TCNNQ vs Alpha-Sexithiophene/F6TCNNQ, J. Phys. Chem. C. 122 (2018) 18705–18714. doi:10.1021/acs.jpcc.8b03744.

[3] J. Stöhr, D. Outka, Determination of molecular orientations on surfaces from the angular dependence of near-edge x-ray-absorption fine-structure spectra, Phys. Rev. B. 36 (1987) 7891–7905. doi:10.1103/PhysRevB.36.7891.

[4] M. Oehzelt, N. Koch, G. Heimel, Organic semiconductor density of states controls the energy level alignment at electrode interfaces, Nat. Commun. 5 (2014) 4174. doi:10.1038/ncomms5174.

[5] M. Oehzelt, K. Akaike, N. Koch, G. Heimel, Energy-level alignment at organic heterointerfaces, Sci. Adv. 1 (2015) e1501127. doi:10.1126/sciadv.1501127.

[6] S. Krause, A. Schöll, E. Umbach, Interplay of geometric and electronic structure in thin films of diindenoperylene on Ag(111), Org. Electron. 14 (2013) 584–590. doi:10.1016/j.orgel.2012.11.023.

[7] A. Wilke, J. Endres, U. Hörmann, J. Niederhausen, R. Schlesinger, J. Frisch, P. Amsalem, J. Wagner, M. Gruber, A. Opitz, A. Vollmer, W. Brütting, A. Kahn, N. Koch, Correlation between interface energetics and open circuit voltage in organic photovoltaic cells, Appl. Phys. Lett. 101 (2012) 233301. doi:10.1063/1.4769360.

[8] F. Zhang, A. Kahn, Investigation of the High Electron Affinity Molecular Dopant F6-TCNNQ for Hole-Transport Materials, Adv. Funct. Mater. 28 (2018) 1703780. doi:10.1002/adfm.201703780.